DETERMINATION OF THE CURIE POINT DEPTH OF ANAMBRA BASIN AND ITS ENVIRONS USING HIGH RESOLUTION AIRBORNE MAGNETIC DATA

Christopher Aigbogun & Kuforijimi Olorunsola
Department of Physics, Faculty of Physical Science, University of Benin, Benin City

ABSTRACT
The subsurface of Anambra basin was assessed for geothermal energy source which is a renewable energy using airborne magnetic data. Gridded data of digitized twelve (12) airborne magnetic maps of high resolution were acquired from the Nigerian Geological Survey Agency, Abuja for this research. The data were combined to form a composite map - total magnetic intensity (TMI) anomaly map. Regional-residual separation of the total magnetic intensity data was performed using Polynomial Fitting method. The filtered residual data was Fourier transformed after dividing the whole area into Thirty-five (35) overlapping cells for spectral analysis. The subsurface geology of the study area was delineated into shallow and deeper sources. Spectral analysis for crustal magnetization was used for the determination of the depth to magnetic sources giving rise to magnetic anomalies for the determination of; curie point depth and geothermal heat flow supply. Conclusively, the results show that the study area has good sedimentary thickness with the highest value of 3.86 km, Curie point highest value was 38.62 km and geothermal heat flow highest value was 99.02 mWm^{-2} around Aimeke, Enugu, Mbashere, Ankpa and Ogobia. Due to the moderate to low Curie point depths, there was no anomalous geothermal heat flow in the study area, thus, the basin has a likelihood of geothermal heat flow prospect.

Keywords: *Airborne; Magnetic; Curie Point Depth; Heat Flow; Spectral Analysis; Regional-Residual.*

1. INTRODUCTION
Airborne magnetic data was used to determine the Curie point depth and the heat flow potentiality of the Anambra basin, Nigeria. In the work of Artemieva *et al* [1] it was established that the distribution of temperature within the earth is one of the most significant parameters used in earth sciences for accurate calculation of Curie point depth (CPD) to estimate the geothermal heat flow information of the subsurface as it relates to Anambra basin. The top and bottom of the magnetized crust will be calculated using the Power-Density spectra of the total magnetic field from the airborne magnetic data. Ross *et al*. [2] also affirmed that Curie point depth depends largely on the magnetic minerals and in general 580ºC will be used as Curie temperature in the continental crust. According to Bansal *et al*. [3] the basal depth of the magnetic sources can be caused by disparities in lithology, the depth to the bottom of magnetic sources (DBMS) and Curie point depth do not necessarily correspond.

2. GEOLOGICAL BACKGROUND OF THE STUDY AREA
The area of study is bounded by latitudes 7°00' and 9°00' North and longitudes 6°00' and 7°30' East of the Southern part of Anambra basin and presented in figure 1 The Anambra basin is an elongated NE – SW trends and is located at the south-western fringe of the Benue Trough bordered on the west by the Precambrian basement complex rocks of western Nigeria and on the east by the Abakaliki Anticlinorium. In the geological settings research carried out by Petters. [4] the Asu River Group in the Anambra basin consists of shales, limestones and sandstone lenses of the Abakaliki Formation in the Abakaliki area and the Mfamosing Limestone in the Calabar Flank. The Sedimentation in the Lower Benue Trough started with the marine Albian Asu River Group, even though some pyroclastics of Aptian – Early Albian ages have been scarcely reported by Ojoh. [5] The stratigraphic succession of the Benue Trough showing Anambra basin is presented in figure 2
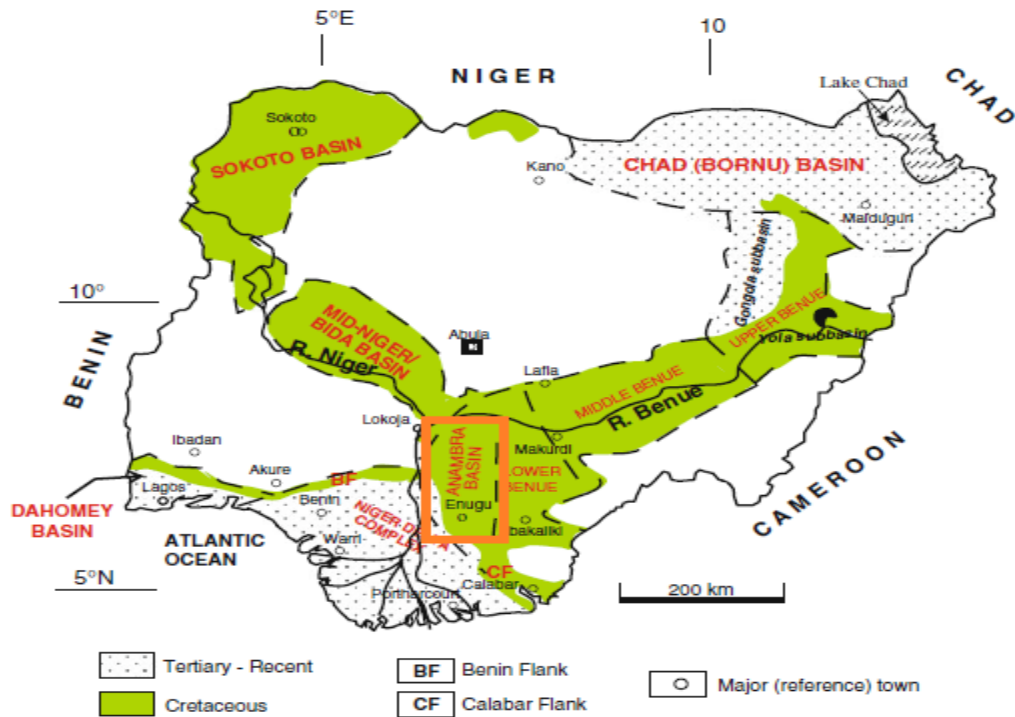
Figure 1: Generalized geological map Nigeria showing the study area in Red Rectangle. [6]
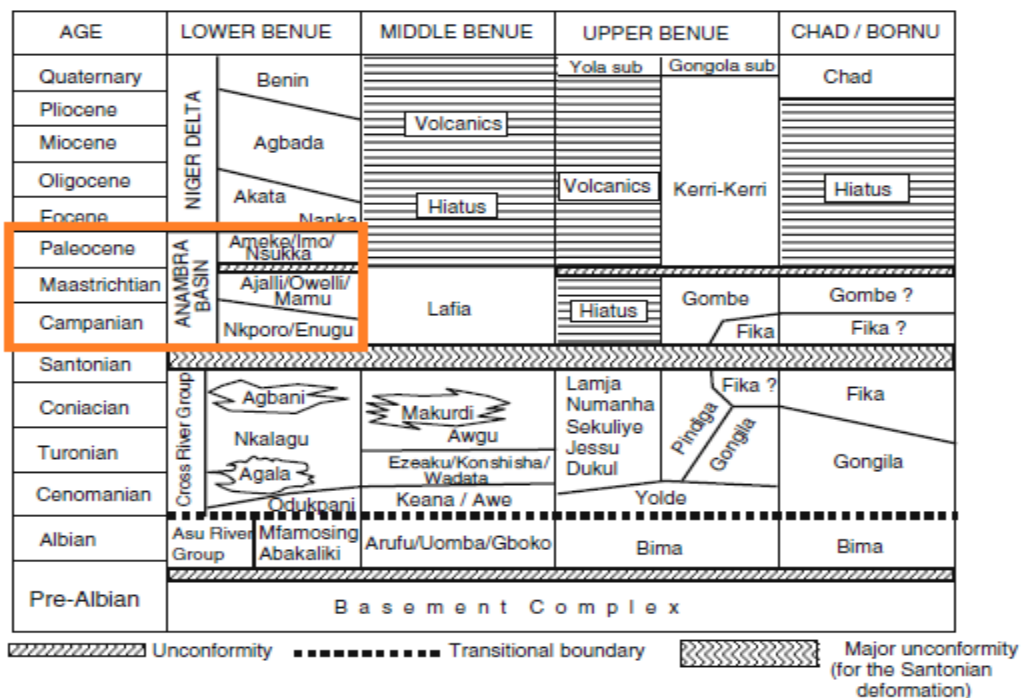

Figure 2: Stratigraphic successions in the Benue Trough highlighting Anambra Basin in Rectangular Block and the Nigerian sector of the Chad Basin. [6]

3.   MATERIALS AND METHODS

3.1   Data Acquisition

Twelve (12) sheets of aeromagnetic data of number 268, 269, 270, 271, 287, 288, 289, 290, 301, 302, 303 and 304 of very high-resolution covered the study area. They were measured and acquired between 2004 and 2008 on a scale of

1: 100,000 series by Fugro Airborne Surveys for Nigerian Geological Survey Agency (NGSA). The sheets were used as basic data for determining the nature of magnetic anomalies over the area. The survey was carried out along a series of North-South lines with a spacing of 2 km and an average flight elevation of 80 m above the sea level. The magnetic data was obtained from digitization of the total magnetic intensity contour maps at an interval of 0.0271 units at a flight line spacing of about 3 km.

3.2   Airborne Magnetic Data Processing

The gridded data were merged and fed into Oasis Montaj version 8.3" to produce a composite map – total magnetic intensity anomaly map. The data is in three columns: latitude, longitude and magnetic values. The magnetic data was reduced to the equator using a Butterworth low-pass filter to produce reduction to the equator total magnetic intensity anomaly map (figure 3) with certain standard parameters: geomagnetic inclination of -8.571°, geomagnetic declination of -1.779°, and amplitude correction of -20, while the Butterworth low-pass filter parameters include: cut-off wavelength of 500 m and filter order of 8. The -8.571° and -1.779° are mean values of the geomagnetic inclination and declination, computed for the area based on the IGRF-11 model for year 2006–2007 as adopted by the International Association of Geomagnetism and Aeronomy (IAGA) (NOAA/NGDC; [7]   Anudu *et al*; [8] Rajagopalan; [9] Wijins *et al*. [10]

The reduction to the equator converts the composite map into one with better directions of magnetization field.

The RTE-TMI data was separated into two components: residual and regional. This research is focused on the residual magnetic data and the anomaly map produced (figure 4). The area is now divided into thirty-five (35) overlapping cells for spectral analysis. The spectral energies versus their corresponding wave-numbers were plotted (figure 5). The values of the deeper and shallow magnetic source depths were calculated by written a program in MATLAB.
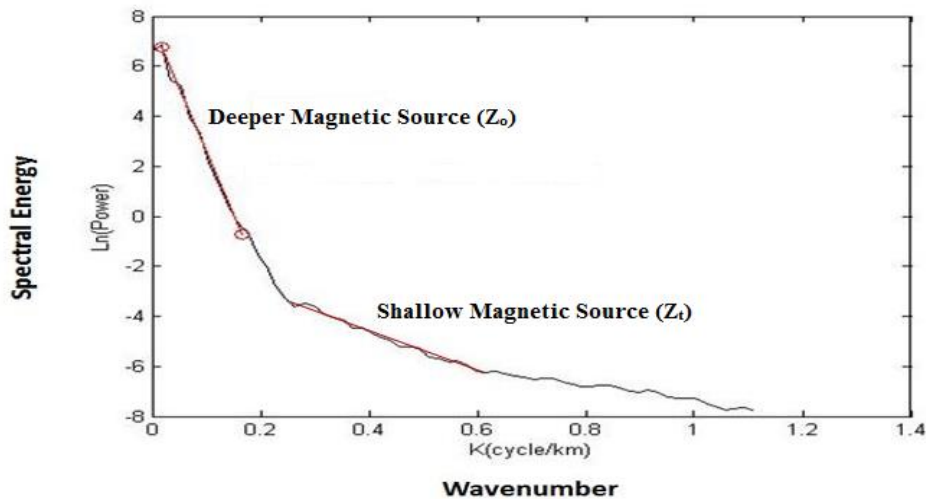

Figure 3: Typical Plot of spectral energy against wave-number showing deeper magnetic source depths

Spector and Grant; [11] Blakely [12] presented the power spectrum, P, for a 2D assemblage of bodies can as follow.

$$P(k_x k_y) = 4\pi^2 c_m^2 |\Theta_m|^2 |\Theta_f|^2 e^{-2|k|zt}(1 - e^{-|k|(zo-zt)})^2 \qquad (1)$$

The parameters below have once been used by Cianciara and Marcak; [13] Nafiz [14] in their research work to estimate Cuire Point Depth. Here, k_x and k_y are the wavenumbers in the x- and y-axes; C_m is a constant of proportionity; ϕ_m is the power spectrum of the magnetization; Θ and Θ_f are the directional factors related to the magnetization; Θm and Θf geomagnetic field, respectively; and z_t and z_o are the top and bottom depths of the magnetic sources.

After annual average, equation (1) can be written as

$$P(|k|) = A_1 e^{-2|k|zt} (1 - e^{-|k|(zo-zt)})^2 \qquad (2)$$

Where A_1 is a constant Equation (2) can be simplified to compute the shallow depth Z_t of the magnetic source as previously used by Spector and Grant; [11] Bhattacharyya and Leu; [15] Okubo *et al*; [16] Abraham *et al*; [17] from the low-wavenumber part of the power spectrum as follows:

$$\ln\left(\frac{P(|k|)^{1/2}}{|k|}\right) = \ln A_2 - |k|z_o \qquad (3)$$

Here, ln is the natural logarithm and A_2 is a constant depending on the properties of magnetization and orientation. Equation (2) is also simplified to compute the top of magnetic sources (z_t) by assuming that the signals from the source

tops dominate the spectrum. Tanaka *et al.* [18] established that for wavelengths less than about twice the thickness of the layer, equation (2) approximately becomes:

$$\ln[P(|k|)^{1/2}] = \ln A_3 - |k| z_t \tag{4}$$

The estimated Curie point depth is performed in tow steps: the first is to calculate the (z_o) of the shallow magnetic sources using equation (3) and the second is to calculate the (z_t) of the deeper magnetic sources using equation (4). This approach is known as centroid depth method by Bansal *et al.* [3] Bhattacharyya and Leu. [15] derived the equations for calculating the centroid and top depths for 2D structures with arbitrary polygon cross-sections. Okubo *et al* [16] suggested that the same equations are applicable to any 3D shaped bodies. The Curie point depth can be calculated as follows:

The Curie point depths were calculated using equation (5) gotten from the values of the deeper and shallow magnetic source depths calculated from the residual magnetic data using equations (3 & 4).

$$Z_b = 2Z_O - Z_t \tag{5}$$

The value of the Geothermal heat flow is expressed by Fourier's Law with equation

$$q = [\frac{dT}{dT}]\lambda \tag{6}$$

Tanaka et.al; [18] Tanaka and Ishikawa; [19] used the same equation to calculate geothermal heat flow, where (q) is the geothermal heat flow, (λ) is the coefficient of thermal conductivity. Reiter *et al* [20] carried out the thermal conductivity of all lithology and 2.5 $Wm^{-1}\,^{o}C^{-1}$ was taking as an average of Thermal conductivity value because of the predominant lithology in this area is Shale.

The Curie temperature (θ) can be obtained from the Curie point depth (Z_b) and the thermal gradient $(\frac{dT}{dZ})$ using the following equation;

$$\theta = [\frac{dT}{dT}]Z_b \tag{7}$$

The geothermal heat flow values were calculated by combining equations (6) and (7)

$$q = \lambda[\frac{\theta}{Z_b}] \tag{8}$$

4. RESULTS OF THE ANALYSIS

The results are presented in tables and Figures for a clear understanding. Tables 1 - 2 show the shallow and deeper magnetic sources derived from the power-density Spectra Energy of the study area. While table 3 shows the Curie point depth. The shallow magnetic source represents the depth of the sediment and it is up to 3.86 km in the study area which is a good indication of hydrocarbon prospect.
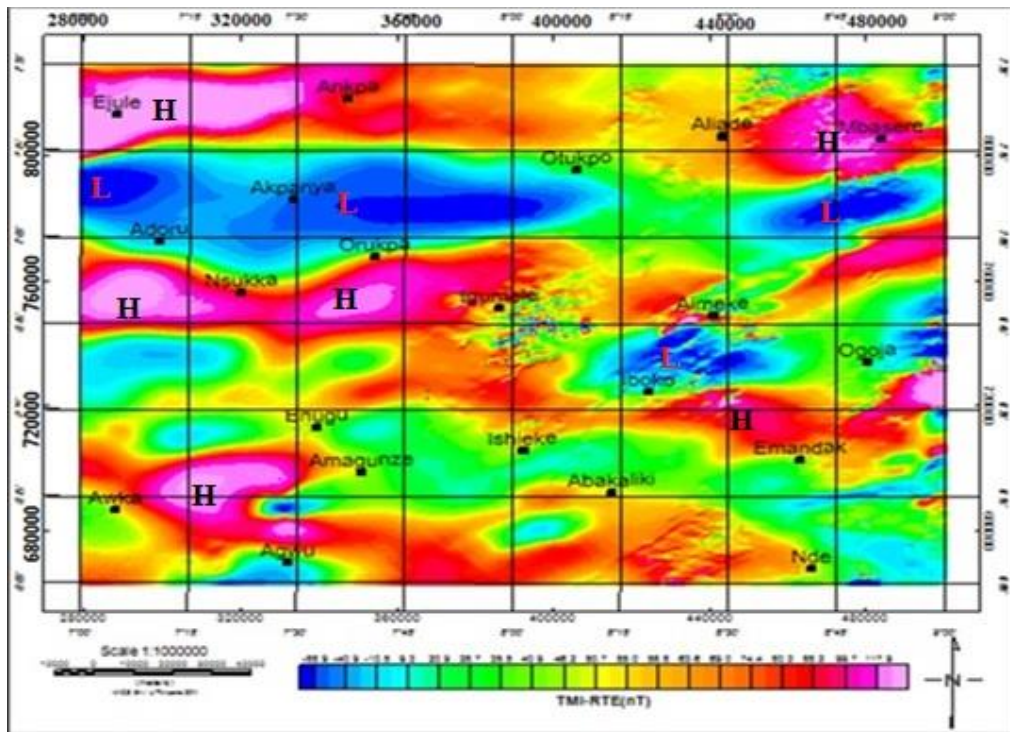

Figure 4: Reduction to the Equator of Total Magnetic Intensity (RTE-TMI) Anomaly map of the study area.
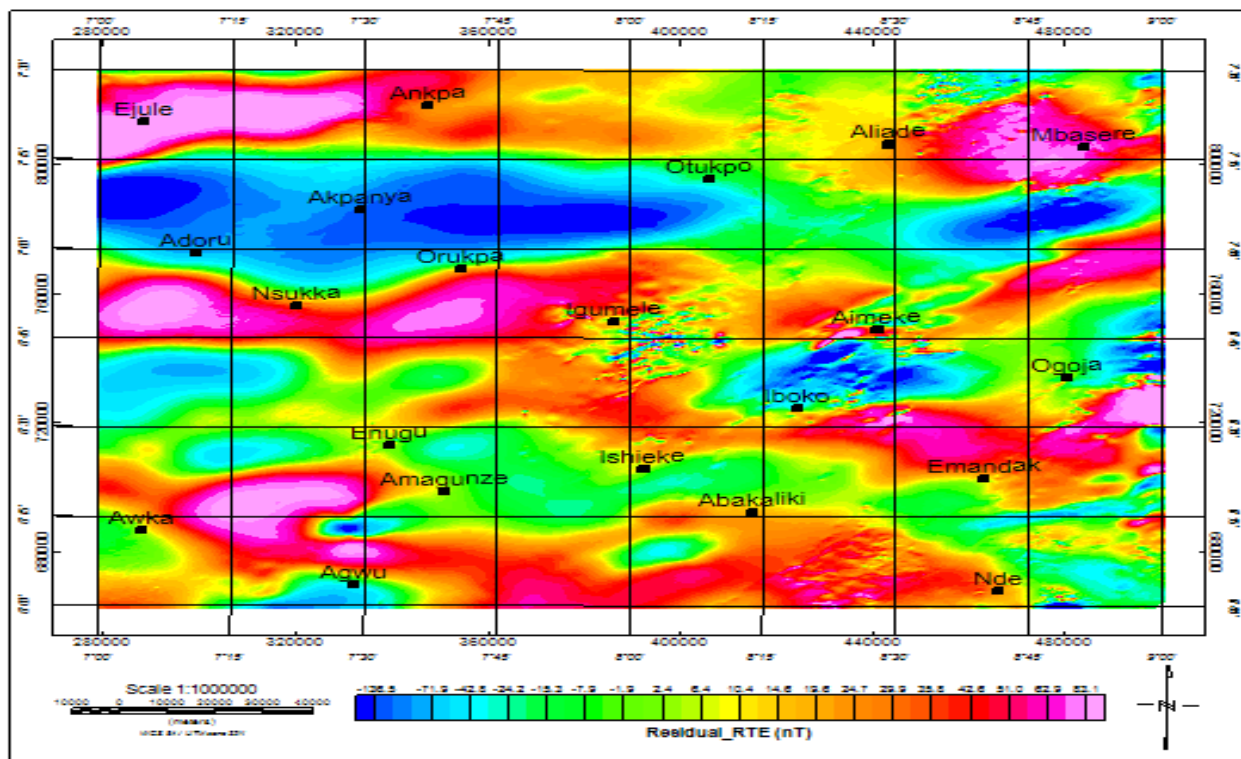
Figure 5: Residual Magnetic Field Map of the Study Area. The x- y-axes are longitude and latitude coordinates in decimal degree with some magnetic closures respectively. Unit of residual magnetic field = nano Tesla

Table 1: Estimated depths to the deeper (Z_o) and shallow (Z_t) magnetic sources in km

Cells	Latitude(º)	Longitude(º)	Shallow Source (Z_t) km	Deeper Source (Z_o) km	Curie Point Depth (Z_b) km	Heat Flow mWm^{-2}
1	6.25	7.25	3.57	10.37	17.16	84.50
2	6.25	7.50	2.43	9.51	16.60	87.36
3	6.25	7.75	1.41	8.03	14.64	99.02
4	6.25	8.00	1.04	10.24	19.44	74.58
5	6.25	8.25	1.18	12.65	24.12	60.13
6	6.25	8.50	1.28	13.67	26.06	55.64
7	6.25	8.75	1.22	9.52	17.40	81.37
8	6.50	7.25	1.08	12.38	23.69	61.22
9	6.50	7.50	0.98	10.14	19.31	75.10
10	6.50	7.75	1.50	9.48	17.47	82.99
11	6.50	8.00	0.81	10.74	20.66	70.17
12	6.50	8.25	1.17	9.68	18.18	79.75
13	6.50	8.50	1.13	10.19	19.25	75.32
14	6.50	8.75	1.01	8.01	16.02	96.57
15	6.75	7.25	0.59	17.32	34.04	42.60
16	6.75	7.50	3.86	16.23	28.60	50.69
17	6.75	7.75	1.53	15.85	30.18	48.05
18	6.75	8.00	1.43	11.31	21.19	68.43
19	6.75	8.25	1.30	10.98	20.65	70.21
20	6.75	8.50	1.43	11.08	20.73	69.94

21	6.75	8.75	1.71	8.44	15.18	95.55
22	7.00	7.25	1.00	13.48	25.97	55.84
23	7.00	7.50	2.08	17.20	32.33	44.85
24	7.00	7.75	1.07	19.85	38.63	37.54
25	7.00	8.00	1.11	15.87	30.63	47.34
26	7.00	8.25	1.12	11.32	21.52	67.37
27	7.00	8.50	1.67	9.90	18.13	79.99
28	7.00	8.75	0.94	10.35	19.76	73.36
29	7.25	7.25	0.81	11.79	22.76	63.70
30	7.25	7.50	0.99	14.09	27.21	53.29
31	7.25	7.75	1.34	10.27	19.19	75.56
32	7.25	8.00	1.44	11.35	21.27	68.18
33	7.25	8.25	1.27	12.12	22.96	63.15
34	7.25	8.50	0.94	11.47	22.01	65.89
35	7.25	8.75	0.97	14.05	27.13	53.45

4.1   Relationship between Curie Point Depth and Heat Flow

The residual data was now used for the calculation of the depth the Curie point depth and the heat flow for the study area. In order to investigate any possible relationship between Curie point depth and heat flow, the values of the Curie point depth with their corresponding geothermal heat flow were plotted. The corresponding surface heat flow values were calculated using Curie-point temperature of 580 ºC and thermal conductivity of 2.5 $Wm^{-1}ºC^{-1}$. The geothermal heat flow map of the study area was presented in (Figure 6).
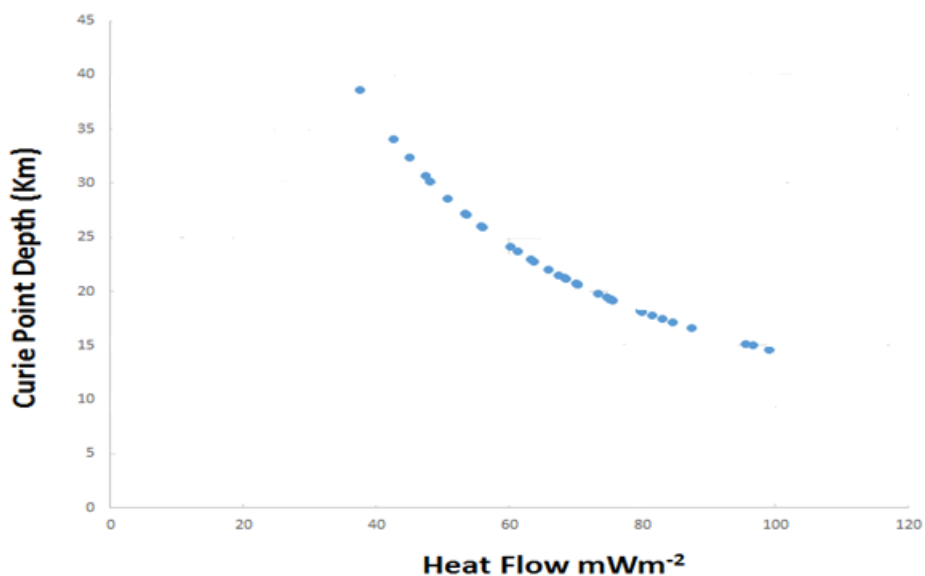

Figure 6: The Curie point depth versus Heat flow data graph of the study area.
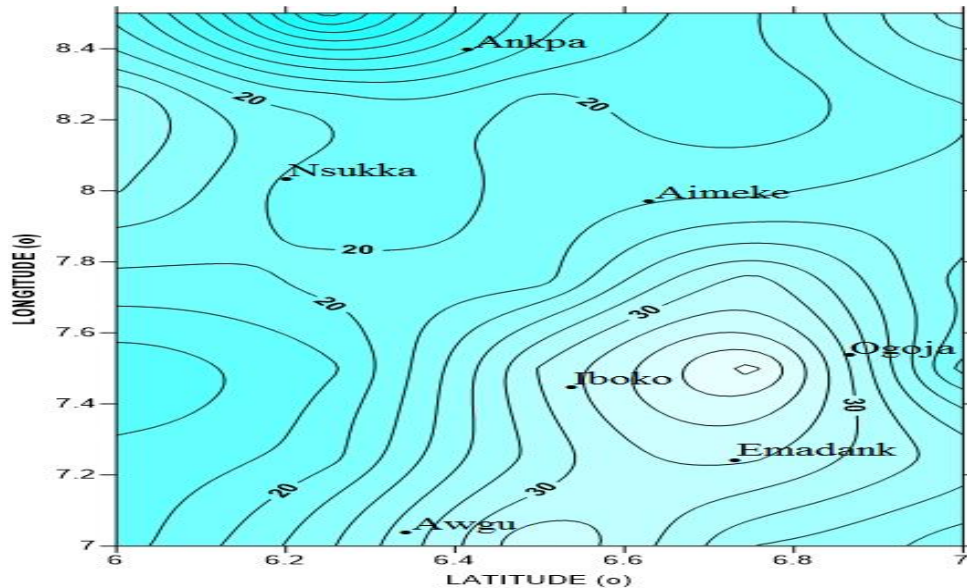
Figure 7: Curie Point Isotherm Map in km. (Contour interval is 2.0 km)

5.   DISCUSSION

The magnetic highs are shown in red colours denoted with "H" and magnetic lows in blue colours are denoted with "L" (Figure 4). The low magnetic values represent the area where the anomaly is deeply seated. After the regional-residual separation, the maps of the output are shown in (Figures 4 & 5). Considering Curie point depth and heat flow in the study area as shown in Figure 6, it is clear that the heat flow increases with decrease in curie point depth. The graph of Heat flow (q) versus Curie point depth (Z_b) values, shows that they are proportional.

The Curie point depth ranges from 14.64 km and 38.62 km and the geothermal heat flow values ranges from 37.54 to 99.02 mWm^{-2} The heat flow values here does not exceed 100 mWm^{-2}. This shows that there is no anomalous heat flow in the study area. High Curie point depth values are observed around Iboko, Ogoja and Emadank areas with consequent low geothermal heat flow values. While low Curie point depth is observed around Aimeke, Awgu, Nsuka and Ankpa area mixed with both basement complex and sedimentary rocks. The low Curie point depth area shows high geothermal heat flow values. The high heat flow at low Curie point depth shows that the mantle is close to the surface where the basement complex is found. Therefore, the geothermal heat source is close to the surface. Jessop *et al* [21] carried out the standard geothermal heat flow values of all regions which mentioned that 60 to 100 mWm^{-2} is considered to be prospective heat flow values.

6.   CONCLUSION

Based on the results from the low values of the Curie point depth in some areas, there is likelihood that the study area has geothermal energy potentials. The geothermal heat flow values around Enugu, Awgu and Aimeke fall between 60 and 100 mWm^{-2} which is the acceptable standard for geothermal heat flow potentiality. The lower values of Curie point depth in these areas show a moderate value for the subsurface geothermal heat flow. Comprehensive ground magnetic survey should be carried out in Aimeke, Enugu and their environs to ascertain the prospect of these areas for geothermal energy production.

7.   REFERENCES

[1].   I.M. Artemieva, W.D. Mooney. Thermal Thickness and evolution of Precambrian Lithosphere, A Global Study Journal of geophysics Research. 106(B8), 16,387 & 16,414,doi:10.1029/2000 JB900439 (2001).

[2].   H.E. Ross, R.J. Blakely, M.D. Zoback. Testing the use of aeromagnetic data for the determination of Curie depth in California. Geophysics; (71): p.51–59 (2006).

[3].   A. R. Bansal, G. Gabriel, V.P. Dimri, C.M. Krawczyk. Estimation of depth to the bottom of magnetic sources by a modified centroid method for fractal distribution of sources: an application to aeromagnetic data in Germany. Geophysics; 76: L11–L22 (2001).

[4].   S.W. Petters. Centralwest African Cretaceous-Tertiary benthic foraminifera and stratigraphy. Palaeontographica Abt A; (179):1–104 (1982).

[5]. K.A. Ojoh. The Southern part of the Benue Trough (Nigeria) Cretaceous stratigraphy, basin analysis, paleo-oceanography and geodynamic evolution in the equatorial domain of the South Atlantic. NAPE Bull; 7:131–152 (1992).

[6]. N.G. Obaje. Geology and mineral resources of Nigeria. Berlin: Springer Publishers; p.203 (2009).

[7]. NOAA/NGDC. World Magnetic Model – Epoch 2010: Main Field Inclination. National Oceanic and Atmospheric Administration (NOAA)/National Geophysical Data Centre (NGDC), Colorado USA (2010).

[8]. G.K. Anudu, A.S. Randell, I.M. David. Using high resolution aeromagnetic data to recognize and map intra-sedimentary volcanic rocks and geological structures across the Cretaceous middle Benue Trough, Nigeria. Journal of African Earth Sciences; p.625–636 (2014).

[9]. S. Rajagopalan. Analytic signal vs. reduction to pole: solutions for low magnetic latitudes. Explor. Geophys; 34 (4), p.257–262 (2003).

[10]. C. Wijins, C. Perez, P. Kowalezyk. Theta map: Edge Detection in Magnetic Data. Geophysics; (70): p.L39-L43 (2005).

[11]. A. Spector, F.S. Grant. Statistical models for interpreting aeromagnetic data. Geophysics; (35), p.293-302 (1970).

[12]. R.J. Blakely. Potential Theory in Gravity and Magnetic Applications. 1st Ed. Cambridge, UK: Cambridge University Press; (1995).

[13]. B. Cianciara, H. Marcak. Interpretation of Gravity Anomalies by means of Local Power Spectra. Geophysical Prospecting. (24), p.273-286 (1976).

[14]. Nafiz Maden. Crustal Thermal Properties of the Pontides (Northern Turkey) Deduced from Spectral Analysis of Magnetic Data. Turkish J of Earth Sci. Vol.18, p.383-392 (2009).

[15]. B.K. Bhattacharryya, L.K. Leu. Analysis of magnetic anomalies over Yellowstone National park mapping the curie-point isotherm surface for geothermal reconnaissance. Journal of Geophysics Research. 1975 (80); p.4461-4465 (1975).

[16]. Y. Okubo, R.J. Graft, R.O. Hansen, K. Ogawa, H. Tsu. Curie point depths of the Island of Kyushu and surrounding areas, Japan. Geophysics; (53): p.481–494 (1985).

[17]. E.M. Abraham, E.G. Obande, M. Chukwu, C.G. Chukwu, M.R. Onwe. Estimating depth to the bottom of magnetic sources at Wikki Warm Spring region, northeastern Nigeria, using fractal distribution of sources approach. Turkish J of Earth Sc. (24) (2015).

[18]. A. Tanaka, Y. Okubo, O. Matsubayashi. Curie point depth base on spectrum analysis of the magnetic anomaly data in East and Southeast Asia. Tectonophysics; (306): p.461-470 (1999).

[19]. A. Tanaka, Y. Ishikawa. Crustal thermal regime inferred from magnetic anomaly data and its relationship to seismogenic layer thickness: The Japanese islands case study. Physics of the Earth and Planetary Interiors; (152): p.257-266 (1999).

[20]. M.A. Reiter, A.M. Jessop. Estimates of terrestrial heat flow in offshore Eastern Canada. Canadian Journal of Earth Sciences; (22): 1503–1517 (1985).

[21]. A.M. Jessop, M.A. Habart, J.G. Sclater, JG. The World heat flow data collection 1975. Geothermal services of Canada. Geotherm Services. (50), p.55-77 (1976).